Basic RF and Microwave Measurements: a Review of Selected Programs

A. J. Estin, J. R. Juroshek, R. B. Marks, F. R. Clague and J. Wayde Allen

Abstract. This paper* summarizes the principles, historical background and present status of three primary areas of rf and microwave measurements and standards: circuit parameter measurement, power measurement, and noise generation and measurement. Both the reference standards and the techniques of measurement and of transfer to secondary standards are addressed. An extensive bibliography is provided to enable the interested reader to pursue areas to greater depth, and brief discussions to indicate likely directions of current and future work are included.

1. Microwave Circuit Measurements (J. R. Juroshek and R. B. Marks)

1.1 Introduction

The automatic network analyzer (ANA) has become an indispensable tool for the modern microwave engineer. Measurements that were inconceivable twenty years ago can now be performed in seconds. The combination of the network analyzer and the computer has been particularly valuable in providing new tools for modeling, measuring, and analyzing systems and components. The purpose of this section is to review some of these developments.

1.2 Network analyzer technology

The most significant advancement in microwave measurement technology during recent years has been the development of the wide bandwidth automatic network analyzer (ANA) that measures both the magnitudes and phases of network parameters. These vector quantities are measured rapidly at many frequencies over wide bandwidths, automatically corrected for instrument errors, stored, and presented in a variety of different formats. Vector ANAs that can make measurements from 40 MHz to 60 GHz in coaxial waveguide, with a single test set, are now available. Optional waveguide test sets that extend the operating range to frequencies above 100 GHz are available.

Significant advancements have been made in the computers and software that are used with these analyzers. Software for calibration (sometimes called "accuracy enhancement") has been particularly successful at increasing the overall measurement accuracy of the network analyzers. The combination of the wide bandwidth ANAs and time domain software is powerful and has greatly expanded the capabilities for microwave measurements.

Most commercial network analyzers are constructed using 2-stage heterodyne principles [1]. A simplified block diagram of a heterodyne network analyzer is shown in Figure 1. The first stage of the analyzer typically down-converts the signal to an IF frequency near 20 MHz, while the second stage down-converts to an IF frequency usually between 100 kHz and 300 kHz. The magnitudes and phase relationships of the input rf signals are maintained throughout the frequency conversion. After frequency conversion, the input rf signals are detected in quadrature synchronous detectors, and the voltage outputs from the quadrature detectors are digitized for subsequent computer processing.

Another type of network analyzer is the six-port [2-6]. This is the type of network analyzer that has been used at the NIST for most of its calibration activities. In contrast to a heterodyne analyzer, the

A. J. Estin: CyberLink Corporation, 1790 30th Street, Suite 300, Boulder, CO 80301, USA.
J. R. Juroshek, R. B. Marks, F. R. Clague and J. Wayde Allen: National Institute of Standards and Technology, Boulder Laboratories, 325 Broadway, Boulder, CO 80303, USA.

metrologia
Metrologia 1992, 29, 135-151

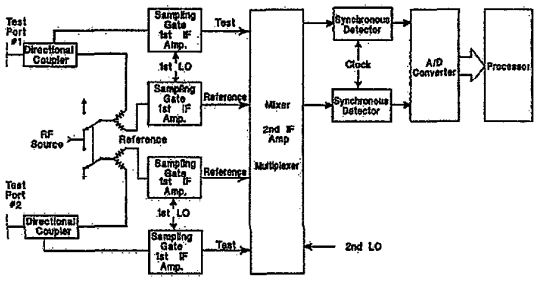

Figure 1. Block diagram of a heterodyne ANA.

six-port uses homodyne detection and intrinsically corrects for imperfect directivities, mismatches, and so on, in its components. While there are a number of different designs for six-ports, most are similar to that shown in Figure 2. The input signal in Figure 2

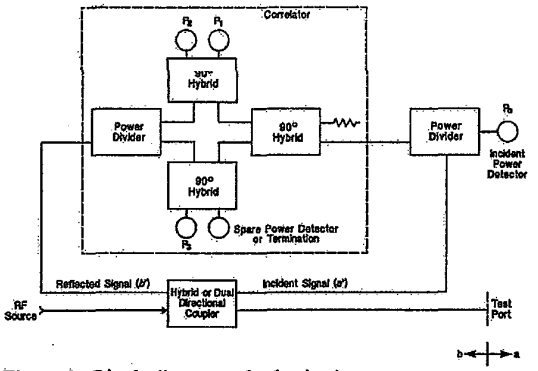

Figure 2. Block diagram of a basic six-port.

is first sent to a 90° or 180° hybrid. That hybrid (a dual directional coupler can also be used) splits the signal, sending half to the test port and the other half to the power detectors. Similarly, any reflected signal from the test port returns to the hybrid where it also splits, with one part going to the power detectors and the other back to the input source. The combination of the incident and reflected signals is measured in power detectors P_0, P_1, P_2, and P_3. Power detector P_0 measures only incident signal, while the other three detectors measure a combination of both incident and reflected signals.

A major component of the six-port is the correlator, a device commonly used to obtain phase information from power measurements [7]. The function of the correlator is to take the two complex signals a' and b' which are ideally proportional to the incident and reflected waves at the test port, a and b, and combine them in such a way to give four outputs which are proportional, respectively, to $(a'+b')$, $(a'-b')$, $(a'+\mathrm{j}b')$ and $(a'-\mathrm{j}b')$. The reflection coefficient at the test port reference plane is given by

$$\Gamma = \frac{\Sigma_i (c_i + \mathrm{j}s_i) P_i}{\Sigma_i \alpha_i P_i}, \qquad (1)$$

where the c_i, s_i, and α_i are constants that are functions of the six-port hardware [7]. These constants are determined during the six-port calibration or error correction. The calibration phase will be further discussed below.

Most of the six-port network analyzers that have been developed at the NIST are dual six-ports [2]. These systems use two six-ports, as shown in Figure 3. A dual six-port network analyzer has a number of advantages over a single six-port. One advantage is its ability to measure the S-parameters of two-port

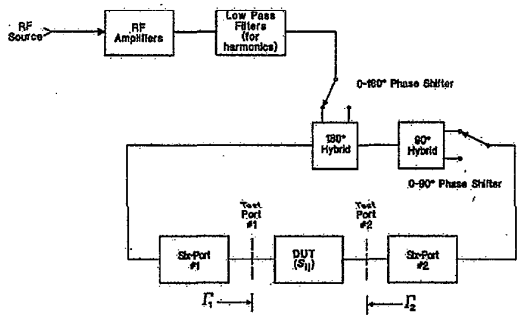

Figure 3. Block diagram of a dual six-port ANA.

devices such as attenuators. As shown in Figure 3, the two six-ports measure Γ_1 and Γ_2 at each end of the two ports. The reflection coefficients, as in Figure 3, and the S-parameters S_{ij} of the device under test (DUT) are related by

$$\Gamma_2 S_{11} + \Gamma_1 S_{22} - S_{11} S_{22} + S_{12} S_{21} = \Gamma_1 \Gamma_2. \qquad (2)$$

Four equations like (2) are generated by changing the phase shifter to each of its four positions, nominally 0°, 90°, 180° and 270°. The S-parameters for the DUT are then determined by solving a set of simultaneous equations.

The procedure outlined above could be duplicated with a single six-port and four offset shorts whose phases differ by 90°. We measure the reflection coefficient of, first, the four offset shorts, and, second, the DUT terminated with the four offset shorts. These measurements also yield the set of four simultaneous equations, given by (2). However, the accuracy of the measurements using the two different methods is not necessarily the same, due to the limited dynamic range of the six-ports. Measurements of high-valued attenuators (40 dB to 60 dB) should be made with a dual six-port, since the accuracy of the measurement would be severely limited by the dynamic range of a single six-port.

1.3 Current six-port technology

Most of the six-port developments have been applied to usage in calibration laboratories [2-6]. This is probably so because the hardware is simple and can be readily realized. In addition to the simplicity of the hardware, another advantage of the six-port is its ability to maintain calibration. Six-ports at the NIST are housed in a temperature-controlled box whose temperature is typically (31 ± 0,05)°C. It is possible to make measurements with those six-ports with calibrations that are more than a month old and still maintain the required uncertainty for the measurements.

The primary disadvantage of the six-port is its relatively low speed. In principle, the measurement speed of a six-port should be faster than a heterodyne ANA since the six-port contains only wide band components, as opposed to the narrower band IF filters in heterodyne ANAs. For maximum accuracy, however, the six-ports at the NIST all use thermistor power detectors which typically require 100 ms or more to stabilize. Thus the time required to measure the reflection coefficient on one of the NIST six-ports is of the order of four seconds per frequency point. In contrast, measurement speeds on heterodyne ANAs are as fast as 200 μs without accuracy enhancement, and 80 ms with accuracy enhancement.

The six-ports that have been constructed at the NIST range in frequency from 10 MHz to 100 GHz. Commercially available 90° and 180° coaxial hybrids are used for the six-port correlators below 18 GHz. Above 18 GHz, the correlators are built with specially fabricated waveguide components. Waveguide-to-coaxial adaptors are used on the waveguide six-port heads for coaxial measurements above 18 GHz. Six-ports have not been developed, to date, with the wide-band frequency coverage typical in a heterodyne analyzer. Measurements from 10 MHz to 40 GHz at the NIST are typically done on four different six-port systems (10 MHz to 1 GHz, 1 GHz to 18 GHz, 18 GHz to 26 GHz, 26 GHz to 40 GHz). The frequency coverage of those systems is dictated largely by the availability of commercial coaxial and waveguide components and thermistor power detectors.

Diode detectors have been used on six-ports with some success [6, 8, 9, 10]. Probably the biggest advantage of diode detectors is their lower power requirement. Diodes typically operate at input powers of 100 μW as opposed to 10 mW for thermistors. Amplifiers in excess of one watt output are used on the dual thermistor six-ports to achieve the desired dynamic range. The dynamic range of the dual six-ports below 18 GHz with thermistor detectors is typically 80 dB. At millimeter-wave frequencies the dynamic range is reduced by 20 dB to 30 dB due to the lack of adequate high power amplifiers. The dynamic range for a heterodyne ANA can be in excess of 100 dB.

One of the problems with using diode detectors on six-ports is their non-square law behavior as the operating power increases. A diode detector only operates as a square law power detector at low power. At higher powers, the diode eventually becomes a linear voltage detector. This deviation from square law is significant, and some type of software correction must be applied to measure power accurately as required by the six-ports [11, 12, 13]. Thus a calibration of the diode is also required for each detector, in addition to the normal network analyzer calibration for accuracy enhancement. Calibration of a diode for deviation from square law is usually done by comparing the diode to a thermistor power detector. Some success has also been achieved in self-calibrating diodes, where one diode is compared with another diode at different power levels to determine the deviation from square law [12]. Diode detectors are also more sensitive to harmonics than thermistor detectors [13]. Harmonics from the rf source as well as harmonics that are generated by the diodes themselves are a significant problem for diode six-ports.

Many of the diode six-ports have been built for pulsed measurements of active devices. The six-port is particularly attractive for pulsed measurements because of its wide band nature. Six-ports with pulse durations as small as 3 μs have been described in the literature [9].

1.4 Network analyzer calibration techniques

All network analyzers have hardware imperfections. Examples of these imperfections are finite directivity in the couplers, imperfect source matches, and reflections due to test ports and cables. Normally these hardware imperfections would severely limit the measurement accuracy of a network analyzer. However, with calibration (accuracy enhancement), the imperfections can be at least partially corrected mathematically by the ANA software, and the measurement accuracy significantly improved.

The software-corrected reflection coefficient Γ_c and the raw or uncorrected reflection coefficient Γ_u in a network analyzer are related by

$$\Gamma_u = \frac{a\Gamma_c + b}{c\Gamma_c + 1}, \tag{3}$$

where a, b, and c are three complex constants. These three constants are the calibration constants and are evaluated when the network analyzer is calibrated. This process requires measuring devices with three or more known values of Γ_c. These devices with known values are the calibration standards. In general, six complex constants are required to characterize a network analyzer with two test ports, three for each

test port. Those six complex constants and the associated software are often called a "12-term error correction model", as they contain six real and six imaginary constants. Once the network analyzer is calibrated, these constants are stored, and the software transformation is applied to each measurement. These constants are frequency-dependent and therefore must be evaluated at each frequency of interest.

A common misconception is that calibration removes all the hardware errors, and therefore the raw uncorrected performance of the ANA is not important. Unfortunately this is not true. It is generally less critical to correct for small hardware imperfections. Serious imperfections usually make the calibration correction larger and therefore more sensitive to time drifts and changes in ambient temperature, as well as to the intrinsic uncertainties. Wideband ANAs usually have larger hardware imperfections than their narrow band counterparts, since extended bandwidth is usually obtained at the expense of performance.

Three measurements of known standards are required in general to perform a calibration of an automatic network analyzer. These can be generated with various combinations of short and open circuit terminations, matched circuit terminations, mismatch terminations, mismatched two-ports, and different lengths of low-loss precision transmission line. The operating software of the network analyzer is designed to make a measurement of each of these devices. The software will then generate correction terms or factors which account for the imperfections in the network analyzer. Thus the bias or errors – resulting from imperfect measuring hardware – can largely be removed.

Several methods have been proposed for calibrating network analyzers [14-17]. Most of the methods are applicable to both heterodyne and homodyne analyzers. These methods are designated by the nature of the standards used in the calibration. Some of these are:

(a) *TRL - Thru, Reflect, Line.* The TRL calibration technique is normally used when high accuracy calibrations are desired. The impedance standard is the line, which in the coaxial case is a beadless air line.

(b) *LRL - Line, Reflect, Line.* The LRL calibration technique is a generalization of TRL where a short length line standard is used in place of the thru. LRL can have wider bandwidth frequency coverage than TRL, as described in the following material. LRL avoids the thru connect whose accuracy may be questionable. However, LRL requires a reference plane translation from the center of the short line standard back to the physical test ports. That translation can introduce additional uncertainties into the calibration.

(c) *TSD - Thru, Short, Delay (Line).* TSD is similar to TRL except that the reflection coefficient of the short circuit termination is assumed to be known.

(d) *TRM - Thru, Reflect, Match.* The TRM calibration technique is similar to TRL except that it uses a matched load in lieu of the line standard. Its advantage is that it avoids the bandwidth limitations of TRL. However, since the reflection coefficient of the match is assumed to be known, TRM introduces inaccuracy unless the match is measured by some other means.

(e) *LRM - Line, Reflect, Match.* The LRM technique is a generalization of TRM in which the thru is replaced by a short length line standard. Using a short line standard instead of a thru introduces advantages and disadvantages as discussed in LRL. LRM and TRM calibration techniques are popular calibration techniques for MMIC measurements.

(f) *TRA - Thru, Reflect, Attenuator.* The TRA technique is similar to TRL except the line standard is replaced with an attenuator of known S-parameters. The major reason for using an attenuator is the avoidance of the bandwidth limitations of a line standard. This technique is not widely used.

(g) *LRA - Line, Reflect, Attenuator.* LRA is simply a variation of TRA where the thru is replaced by a line standard. This technique is also not widely used.

(h) *SSS - Three Different Offset Shorts.* The SSS technique uses three offset shorts to calibrate an ANA. The advantage of using offset shorts for coaxial calibrations is that they are more stable than beadless air lines. Presumably these shorts would be built with a mechanical accuracy comparable to a beadless line standard. This technique has not been widely used.

(i) *OSL - Open, Short, Load.* With the OSL technique, the impedance standard is the load which can be either a fixed load or a sliding load. The reflection coefficient of the short and open are assumed to be known. This technique has received wide acceptance for calibrations that are fast although not always as accurate.

(j) *SSL - Short, Offset Short, Load.* The SSL technique is similar to OSL except the open termination is replaced by an offset short. Offset shorts are preferred for waveguide calibrations since opens are unstable due to their radiation problems. However, the bandwidth of SSL may be limited since the short and offset short may have nearly identical reflection coefficients at some frequencies.

The last three methods are primarily used for one-port calibrations. However, they can be adapted to two-port calibrations by the use of a thru measurement.

Which method to use is dictated by considerations such as the availability of standards, the accuracy desired, and the operating frequency range. How easy a calibration is to use is also an important consideration. The sex of the test-port connectors may also dictate the choice of calibration techniques with coaxial systems. In some cases, a thru connection may not be possible. Some calibrations require that the same reflect standard be connected to both test ports. Connecting the same reflect to both test ports has an advantage in that the value of its reflection coefficient need not be known before the calibration, but can be determined during the calibration process. Connecting the same reflect to both test ports is not possible with sexed mating test ports.

Some general comments about the various calibration techniques are:

(i) Historically the thru connection has been used whenever possible. The assumption is that $S_{11}=S_{22}=0$, and $S_{12}=S_{21}=1$. The validity of this assumption is questionable, particularly with imperfect test ports.

(ii) The reflects used are generally an open and a short circuit. Normally the value of Γ of the reflections need not be known before the calibration. The only requirement is that Γ is the same when connected to test ports 1 and 2. The values for Γ of the reflections are usually determined in the calibration.

(iii) The reflection coefficient of a coaxial open circuit termination, which depends on its fringing capacitance, can be accurately computed, and therefore its value is sometimes entered into the calibration as a known parameter. Open circuits normally are not used in waveguide calibrations since they are efficient antennas and radiate into free space, causing serious and unpredictable errors.

(iv) Fixed air-line standards (beadless air dielectric lines and precise wave guide sections) are generally used for the most accurate calibrations. The assumption made for these standards is that $S_{11}=S_{22}=0$. The values of S_{12} and S_{21} are usually determined by the calibration. One of the problems with coaxial air lines is that the center conductor is free to move about within the tolerance of the test port gaps. Sizeable calibration errors can occur if the test ports have large gaps.

(v) LRL calibrations were generally developed for wide band frequency coverage. The effective length of the calibration standard is $\Delta=L_2-L_1$, where L_1 is the length of the shorter line and L_2 the length of the longer line. The value of Δ can be made as small as desired to extend the frequency coverage to higher frequencies. With TRL, the effective length is simply L_2, because $L_1=0$. The minimum value of L_2 is determined by the minimum electrical length of the coaxial connectors or the waveguide flanges. LRL also avoids the thru validity question described in (i) above.

(vi) The accuracy of a calibration using sliding terminations is generally less than with fixed air-line standards since fixed air-line standards can be manufactured to tighter dimensional tolerances. Sliding terminations have an advantage over fixed air-line standards in that they are easy to use and are particularly suited for single-port calibrations. The accuracy of a sliding termination is determined by the dimensions of the barrel in which the termination slides.

1.5 Impedance standards

Fixed air line standards are used almost exclusively at the NIST for calibration of the six-port network analyzers. Current state-of-the-art manufacturing tolerances for coaxial and waveguide standards are of the order of ± 0,64 μm (25 μin) for the inner conductor diameter and ± 1,27 μm (50 μin) for the outer conductor diameter. Table 1 gives the electrical characteristics of a coaxial air line for the worst case conditions where the inner diameter of the outer conductor is oversized and the outer diameter of the inner conductor is undersized by these amounts. The characteristic impedance of the air line with nonstandard dimensions is denoted by Z, while the line with standard dimensions is Z_0. Table 1 was prepared assuming infinite conductivity for the standards, so that the characteristic impedances are real. The value for S_{11} of an air line is given [18] as

$$S_{11}\sim\frac{(Z-Z_0)}{(Z+Z_0)}(1-e^{-2\gamma\Delta}), \tag{4}$$

where $\gamma=\alpha+j\beta$ is the complex propagation constant and Δ is the effective length as defined in (v) above. The limit on the magnitude of S_{11} is readily obtained from (4) as

$$|S_{11}|\leq 2\left|\frac{Z-Z_0}{Z+Z_0}\right|, \tag{5}$$

which is the value entered in Table 1. The return loss is calculated as

$$R_L=-20\log_{10}(|S_{11}|). \tag{6}$$

In many instances, errors introduced by the connectors equal or exceed the values shown in the table.

Calibration laboratories generally like to have impedance standards with the magnitude of S_{11} less than 0,001. As Table 1 shows, impedance standards with that accuracy are feasible only in the larger lines.

Table 1. Characteristics of a coaxial air line standard with outer conductor diameter 1,27 μm (50 μin) above nominal and inner conductor diameter 0,64 μm (25 μin) less than nominal.

Line size/mm	$(Z-Z_0)/\Omega$	$\lvert S_{11} \rvert$	Return loss/dB
14,29	0,0115	0,00023	72,8
7,00	0,0234	0,00047	66,6
3,50	0,0468	0,00094	60,6
2,92	0,0561	0,00112	59,0
2,40	0,0682	0,00136	57,3
1,85	0,0885	0,00177	55,0
1,00	*0,1638*	*0,00328*	*49,7*

With coaxial air lines, the center conductor is supported solely by the test port connectors and is free to move to and fro within the machining tolerances. With typical test ports that movement can be 0,005 cm (0,002 in) or greater. Normally the center conductor should be positioned at the test port reference planes, causing a gap at both ends of the air line center conductor. If the proper gap is not present, then a calibration error occurs. In actual practice, the placement of the center conductor cannot be controlled and the center conductor is free to move toward one end or the other. Thus one test port is calibrated with too little or no gap, while the other side is calibrated with too much gap. This type of calibration error can be averaged out in a dual six-port, to some degree, by measuring the DUT on both six-ports and then averaging the results.

The optimum calibration frequency for an air line standard is the frequency at which the phase of S_{12} is 90° or some odd multiple thereof (90°, 270°, 450°, and so on). In practice, air line standards are used at frequencies substantially removed from the optimum. When an air line is used to calibrate a network analyzer at a non-optimum frequency, an increase in the systematic error can be expected. However, in many instances that increase is acceptable. The systematic error $\Delta\Gamma$ in the measurement of reflection coefficient Γ is given by

$$\Delta\Gamma = \frac{-S'_{11}}{2\sin\varphi_{12}} e^{-j(\varphi_{12}-90)}, \quad (7)$$

where φ_{12} is the phase of S_{12} of the calibrating airline, and $S'_{11}=S'_{22}$ is the reflection from connector discontinuities on either side of the line [19, 20]. The calibration is ill-conditioned at half-wavelength multiples of line length. This formula is an approximation that is applicable for calibrating with low-loss air lines and measurements of devices with $\Gamma \approx 0$. As an example, the systematic error due to calibrating with an air line with $S'_{11}=0{,}0005$ and $\varphi_{12}=20°$ is $|\Delta\Gamma|=0{,}0007$. Thus a systematic error of 0,0007 can be expected in the measurement of the reflection coefficient of a matched termination. At low frequencies, large values of φ_{12} are difficult to obtain since it is not generally feasible to manufacture precision air lines longer than 30 cm. At the NIST, a 20 cm beadless air line standard has been used for calibrations to frequencies as low as 10 MHz with satisfactory results ($S'_{11}=0{,}0005$, $\varphi_{12}=2{,}4°$, $|\Delta\Gamma|=0{,}006$).

1.6 On-wafer MMIC measurements

Recent growth in the production and use of monolithic microwave integrated circuits (MMICs) has led to new measurement requirements by producers. In order to assess circuit designs and fabrication techniques, improve yields, and promote interchangeability, MMIC developers now require on-wafer measurement of S-parameters. This means that the calibration reference planes must lie in the wafer on which the circuit is constructed. With appropriate test conditions, the analogy to measurements in conventional TEM lines is quite strong, and a number of important techniques carry over with little revision. On the other hand, certain problems as well as opportunities present themselves.

Before the development of on-wafer testing, the conventional method of characterizing an MMIC involved dicing the wafer and mounting the resulting chip in a package. Connections from the chip to external signal ports, typically using coaxial connectors, were made by wire-bonding or similar methods. The resulting packaged device was tested at its external ports using the techniques discussed above. In other words, the MMIC was completely encased in its final packaged form before testing. The cost of packaging, however, is quite high, far exceeding the cost of producing, in large volume, the basic circuit on a wafer. Furthermore, MMIC fabrication typically requires the use of novel and immature technology, so the yield of successful devices is frequently small. As a result, processes which could test at the wafer level, that is, before packaging, were needed so as to avoid the effort and cost of packaging substandard devices.

Although fixtures for testing a diced chip provide a partial solution, dicing is still required and therefore in-process testing is still not feasible. Furthermore, repeatability is suspect. A preferred solution is the use of the coplanar wafer probe. This tool, illustrated in Figure 4, is essentially a coax-to-coplanar waveguide transition. The coplanar end terminates in two or three metallic contacts. In use, these make contact with a coplanar waveguide structure on the wafer, thereby injecting a signal into the waveguide and

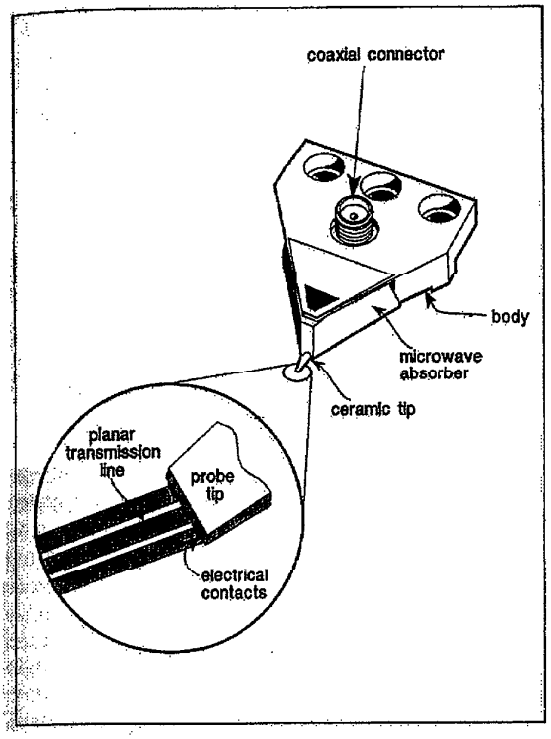

Figure 4. Typical construction of a microwave coplanar wafer probe.

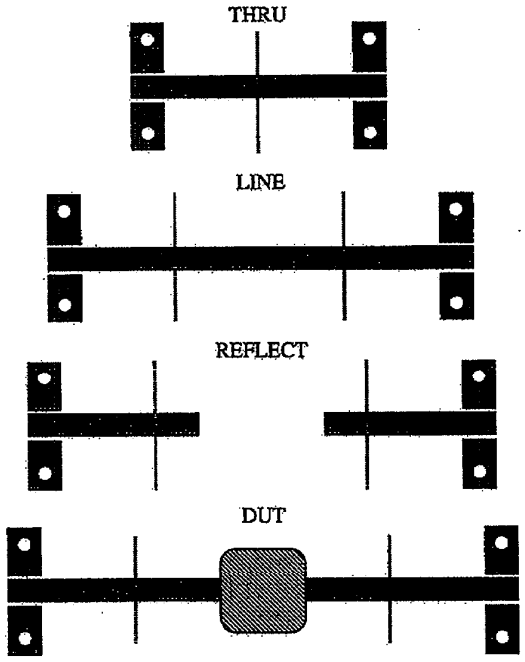

Figure 5. Schematic of on-wafer TRL calibration procedure illustrating reference plane location.

probing the response. Connection to a microstrip line, the other major planar transmission line structure, is somewhat more complicated since the microstrip ground plane lies on the opposite side of the wafer. The conventional approach is to make a metallic connection from the ground plane up to the top surface through a small hole in the wafer, known as a "via".

Assuming that the wafer probes provide a repeatable contact with on-wafer transmission lines (which they typically do), the calibration required for on-wafer S-parameter measurements is similar to that used for coaxial media. The most accurate technique is the TRL method, using two lengths of transmission line (one designated the "thru", the other the "line") as well as an arbitrary symmetric reflective termination known as the "reflect". In the on-wafer case, of course, a direct connection of the test ports is not possible, so the thru standard has finite length. The location of the resulting reference planes corresponds to the center of the thru. The S-parameters of the DUT are measured at these reference planes, as shown in Figure 5.

Although on-wafer S-parameter measurements are in principle similar to those in coaxial cable, several practical differences set the two problems apart. For instance, one minor difference is that, due to the openness of the structure, direct radiative coupling between the probes may affect measurement accuracy. This is not normally a major problem and in any case can be dealt with through shielding. Far more significant is the fact that the planar lines themselves are unique to the fabrication process. Since there are few industry-standard configurations, and since even nominally identical processes can result in significantly different transmission lines, the lines on any two wafers are likely to be quite different. This contrasts to the more conventional transmission line media, in which a small number of well standardized configurations are in common use. The question then arises as to the best source of calibration standards. In contrast to the conventional situation in which the ultimate standards are held by national standards laboratories, the most appropriate on-wafer standards are those built by the device manufacturer to most closely duplicate the transmission lines in use on the DUT. User-produced standards are not only accurate but practical as well, for, unlike the coaxial case, on-wafer standards can be manufactured inexpensively on the same wafer as the devices to be tested.

In addition to being inexpensive to produce, on-wafer standards are easily and rapidly measured using a probe station. This opens the opportunity to introduce additional, redundant standards for improved

calibration. Such a method was recently developed at the NIST [20]. In this method, the additional transmission line standards not only reduce the effect of random connector error but also avoid the bandwidth limitation imposed by the TRL method. The NIST currently uses five transmission lines (including the thru) for calibrations from 0,045 GHz to 40 GHz. Such broad bandwidths are required in many MMIC applications.

Another significant feature of typical planar transmission lines is their great attenuation. Due to the small size (metal thickness of order 1 μm), the loss in the dominant mode may be on the order of 1 dB/cm. The primary consequence of the large loss is through its effect on the characteristic impedance Z_0. The loss not only forces Z_0 to be complex, but also requires it to vary greatly with frequency at wavelengths long enough that the skin depth is comparable to the metal thickness, an important regime for planar lines. Thus, the calculation of Z_0, which is inherently difficult to begin with for a hybrid mode in an open guide of inhomogeneous dielectric, is made even more challenging by the need to fully account for the field penetration into the metal.

Many applications, including those in conventional transmission lines, require a knowledge of the phase of Z_0 which affects the relationship between scattering parameters and power. However, a knowledge of the *magnitude* of Z_0 is particularly important in on-wafer measurements due to the nature of the test devices. For instance, a frequent requirement is the measurement of small, essentially lumped devices connected to the end of a planar line. In order to obtain a measured load impedance that corresponds to the expected low-frequency impedance of such a device, the characteristic impedance of the transmission-line standard needs to be known for it is Z_0 that determines the TRL calibration reference impedance. In contrast, direct measurements of lumped impedances are seldom required in the case of coaxial lines.

In order to deal with the fact that Z_0 is required but is not easily calculated for on-wafer lines, the NIST has developed a method of *measuring* it [21]. A measurement of the propagation constant is required, but such a measurement is a by-product of the TRL calibration. The technique makes use of the relationship between the characteristic impedance and the propagation constant and assumes that the line's capacitance per unit length is a known constant. This approximation is accurate for the quasi-TEM transmission lines which typify interest in this field.

An example of the method is illustrated in Figures 6 and 7. Figure 6 shows the measured Z_0 of a coplanar transmission line. The plotted points were computed by Heinrich [22] using a model of the same line. Although the characteristic impedance is close to its nominal value of 50 Ω at the high end of the band, at the low end the magnitude increases dramatically, and the magnitudes of the real and imaginary parts are nearly equal. As a result, the measured reflection coefficient of a small resistor is complex and frequency dependent when measured by a TRL calibration (Figure 7). On the other hand, having measured Z_0, we are able to transform to a 50 Ω reference impedance, thereby transforming the reflection coefficient to the nearly real, constant value expected of a small resistor. This is indicated in Figure 7.

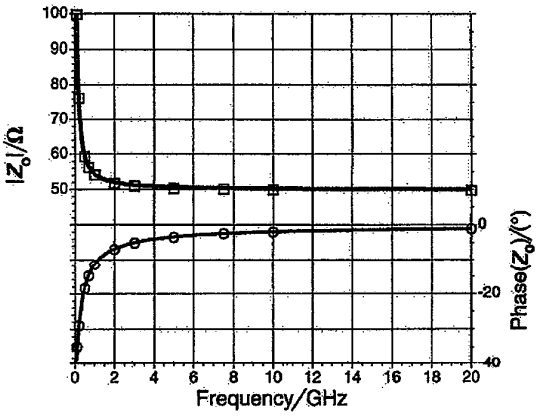

Figure 6. Measured characteristic impedance of a coplanar waveguide line of 0,7 μm gold on 500 μm GaAs. The center conductor is 73 μm wide and the gap width is 49 μm.

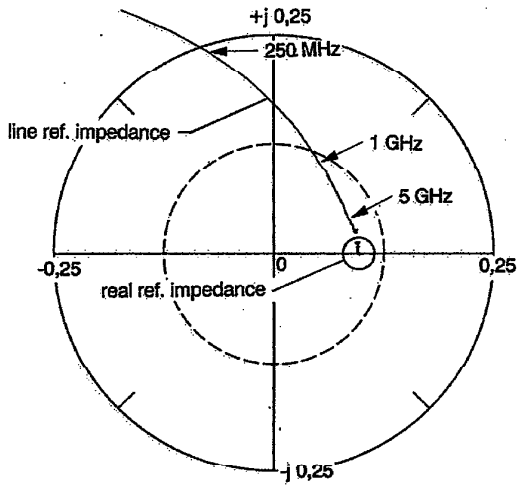

Figure 7. Measured reflection coefficient of a small resistor attached to the transmission line of Figure 6. The curve marked "line ref. impedance" uses Z_0 as the reference impedance; the other uses a reference impedance of 50 Ω.

The measurement described in [21] requires knowledge of the capacitance per unit length of the transmission line. Several procedures for the measurement of this capacitance have been developed [23].

2. Microwave Power
(F. R. Clague and A. J. Estin)

2.1 Microwave power measurement

2.1.1 Methods of power measurement

The microwave point-contact diode has been used for many years for power measurement. Schottky-barrier diodes, however, have better reproducibility and stability, and a lower noise figure. The development of fabrication techniques has led to the widespread use of Schottky-barrier diodes in commercial applications [24, 25]. Improvements in detector mounts and in associated instrumentation have resulted in lower mismatch errors, wider bandwidths covering many decades of frequency up to 50 GHz or more, and high sensitivities, down to nanowatts. Although corrections can be incorporated into microprocessor-controlled power meters, the sensitivity of the Schottky-barrier diode to ambient temperature and its poor linearity preclude its use as a transfer standard. Moreover, the maximum power-handling capacity is quite limited.

Thermoelectric elements, which develop a current in consequence of the absorption of heat from incident rf power, have a high dynamic range (up to 50 dB), can handle relatively high power levels, and are nearly as wide band as diodes. The sensing elements are made in different configurations, such as semiconductor (hot carrier) diodes, thin film devices, and wire elements. However, those that have good wide band characteristics also have poor linearity, and in general are not recommended as transfer standards.

Bolometers are temperature-sensitive resistors, whose change in resistance resulting from the absorption of rf power is determined in some form of resistance-measuring device. These instruments are very nearly linear when used with dc substitution techniques and thus make good transfer standards. Three forms of bolometer are used: barretters, thermistors and thin-film bolometers. Barretters are thin-metal wires which have excellent stability and good sensitivity. They are, however, quite fragile and therefore are not used much outside standards laboratories. A thermistor is a small bead of semiconductor material and is the most widely used bolometer. Film bolometers are physically larger than the others and therefore are usually more useful at lower frequencies and in coaxial systems. The usual form of instrumentation is a bolometer [26] used in conjunction with a self-balancing instrument which automatically controls the dc resistance of the bolometer as the rf power changes [27]. A variety of other forms of rf power measurement such as electron beam interactions, electronic emission phenomena, Hall effect devices and magnetic devices have been developed [28]. These are highly specialized and are not normally used in commercial and laboratory applications.

2.1.2 Correction factors for sensors

Two major error sources must be taken into account when calibrating bolometric measurements. The *equivalence error* results from a distribution of current that is different for the dc power than for the rf power. *Mount efficiency* is the ratio of the rf power absorbed by the bolometer element to the rf power absorbed at the input to the mount. *Effective efficiency* includes both of these errors and is defined as the ratio of dc substituted power to rf power absorbed at the mount input. The magnitude of the equivalence error is usually smaller than that resulting from imperfect mount efficiency, but unlike the latter may be positive or negative. Often a *calibration factor*, which combines effective efficiency with a partial correction for the error caused by power reflection resulting from impedance mismatch, is also determined.

2.2 Power standards

Calorimeters form the basis of primary standards of microwave power measurements and provide the highest quality calibration of other power-measuring devices [29, 30]. They have the advantages that measurements may be referred to fundamental physical quantities, and that the measurement technique can be subjected to a thorough analysis and definitive error evaluation. On the other hand, they are bulky, expensive to construct, require highly trained personnel, slow and difficult to use, have limited dynamic range, and are therefore unsuitable for field use outside the standards laboratory.

Two main types of calorimeter are in primary use at this time, *dry load calorimeters* and *microcalorimeters*, although *flow calorimeters* are also used, particularly for higher power measurements [31]. In the flow calorimeter, in contrast to the dry load calorimeters, heat is removed from the load by circulating a fluid such as distilled water over the load and measuring its temperature rise.

2.2.1 Dry load calorimeters

Dry load calorimeters use a dual input to identical loads in which dc power fed to one load is used to balance rf power absorbed in the other. A sensitive thermopile is used as a thermal null detector between the two loads. The critical part of the measurement system is the design of the loads, which are optimized

to have minimum frequency sensitivity and a very small equivalence error, and to be well matched to one another. Input connectors of the highest quality, that is, having low mismatch and loss, and high repeatability on successive disconnect and connect operations, are necessary. Peltier heating is a source of error in the dc power absorption, but can be cancelled to a first approximation by reversing the direction of current flow in successive measurements. Thomson heating errors cannot be eliminated in this way, but are normally second-order and can be ignored [32]. A technique for evaluating equivalence errors has been described [33] which reduces residual errors to less than 0,01% at 8 GHz. The effects of power absorption and mismatches in the transmission line must be determined and removed from the results.

Dry load calorimeters are useful in both coaxial and waveguide systems, although coaxial systems present a more difficult design problem for the absorbing load. This is so because the absence of an inner conductor in the waveguide simplifies both the configuration of the low reflection load and the heat flow equivalent circuit. In addition, the line losses are lower and the connectors can more closely approach ideal transparency.

Dry load calorimeters have been developed for use in the millimeter wavelength region [34-37].

2.2.2 *Microcalorimeters*

Although the literal meaning of the designation "microcalorimeter" is measurement of low (milliwatt) power, the implication is actually toward a specific instrumentation configuration. It is used to measure effective efficiency, rather than power as such. A bolometric element and its mount are placed in the microcalorimeter. Dc power is applied to bias the bolometer to its proper operating resistance. The dc power and corresponding temperature rise as determined from the thermopile output are recorded. The rf power is turned on and after equilibrium is again achieved, the new dc power and thermopile outputs are recorded. From these measurements, combined with various corrections, the effective efficiency can be calculated. A typical run from a coaxial microcalorimeter is shown in Figure 8. The first and last steps at 109,1 μV are the equilibrium position with only dc power applied, as seen before and after the measurement sequence. The seven intervening steps correspond to the equilibrium conditions at frequencies of 0,1, 1, 5, 10, 15, 17, and 18 GHz, respectively.

A major advantage of this method is that the effects of reflected power due to mismatch and power dissipated in the feed line are eliminated to first order [38]. Thus, the compromises required in thermally isolating lines for dry load calorimeters are largely avoided. In an automated system, with

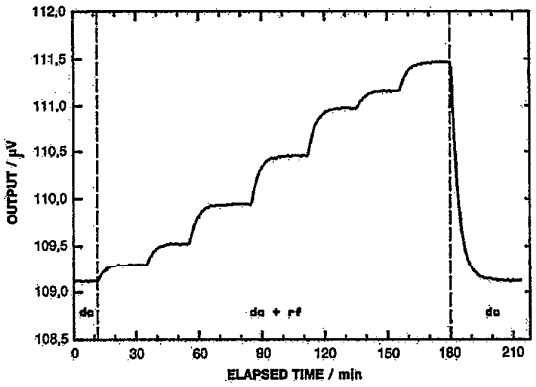

Figure 8. Typical calibration run of a microcalorimeter.

programmable rf sources, digital voltmeters and so on, it is possible to calibrate a bolometer mount in an unattended microcalorimeter. Measurements may be required at a number of frequencies and, since the calorimeter is intrinsically slow in coming to equilibrium, such automation is almost a necessity.

Several sources of error in the microcalorimeter can be either estimated or corrected. The sensitivity of the calorimeter, that is, the ratio of output voltage from the thermopile to the power dissipated in the calorimeter, is different for power which is dissipated in the walls of the mount than for power dissipated in the bolometer element itself. For an effective efficiency of 99%, this changes the effective efficiency by a few parts in 10^4. Experimental techniques for evaluating, and hence for correcting, this error have been developed [39].

Other limiting errors can include [40]: (i) system instabilities over the extended periods of time needed to reach thermal equilibrium; (ii) microwave signal leakage through joints, connectors, or along the dc bias circuit; and (iii) connector nonrepeatabilities, although, at the present state of accuracy determination, this is generally insignificant.

2.3 *Calibration transfer considerations*

2.3.1 *Detector mismatch*

As mentioned in the section on correction factors, the effect of mismatch of a power detector must be removed if its measurements are to be compared with those of a different detector [41]. Consequently, a determination of the power reflected by the detector must be made, usually in terms of its reflection coefficient or input impedance. Early techniques required the use of such tools as the tuned reflectometer [42, 43], which was slow and exacting, and were limited to single-frequency measurements. Adaptations to

untuned reflectometers, which use spacers of precise lengths of waveguide, have simplified the procedures [44, 45], but they are still essentially narrow-band.

More recent developments in automated network measurements have put the entire problem of determining the reflected power into a simpler perspective. Automated network analyzers [46] and six-port procedures [47] enable the user to remove the effects of noise and imperfections in the measuring system from the results, and thereby extend the scope, speed and frequency range of the measurement by many orders of magnitude. Thus, the determination of the reflection coefficient of a power detector and its elimination as a source of error is reduced to a routine procedure.

2.3.2 *Connectors*

A factor which will eventually limit the accuracy with which power meters can be compared is the quality and repeatability of the connector pairs by which the power meter is connected into a system. If a power meter with one configuration of connector is to be used in a system having a different type of connector, the adaptor(s) must be similarly evaluated. Although considerable work has been done in designing precision connectors having low loss, low reflection and high repeatability, and in defining standards for such connectors [48, 49], the experimental determination of the absolute properties of the connector is an extremely difficult task which is not usually attempted. Differential measurements of a connector pair relative to another pair, or relative to itself following disconnection and reconnection, are not useful for correcting measurements of power, and are not considered here.

A direct frequency domain approach [50] to measuring the reflection and losses of a connector pair not only requires high accuracy techniques, but also normally requires another set of connectors which is either of comparable quality and already been evaluated or is so much better that its imperfections can be neglected. Having the evaluated set enables the pair under test to be introduced into the calibrated measurement system. Beatty [50] avoided this difficulty, while measuring a hollow waveguide joint with a precision reflectometer, by sliding the reference standards through the connection under test. His procedure, however, is not usable in a coaxial transmission line. In a power measurement of the highest accuracy, it is presumed that the most nearly ideal available connectors will be used, but the requirement of measuring that "best" connector still remains to be resolved.

Frequency-domain approaches that have been reported by Harris [51] and Estin [52] measure the mismatch and loss of a coaxial connector pair in an indirect way. Although both methods are somewhat limited by their own assumptions and approximations, each yields values for the reflection and insertion loss of the connector pair referred to the characteristic impedance of the line, rather than differentially with respect to another connector pair. Both methods use the fact that the scattering parameters of two discontinuities which are separated in a transmission line by an integral number of guide half-wavelengths superimpose. Neither method can provide continuous measurement over a broad band, for measurements can be made only at those discrete frequencies corresponding to half-wavelength multiples of the line length on which the units under test have been mounted.

Harris [51] has proposed a method for measuring precise coaxial connectors; he assumes that all connectors of a type are identical and describes each connector pair as three cascaded two-ports. He also requires that artifact reference standards (short circuits and matched loads) be known to a high enough accuracy to encompass the imperfections of the connector pair.

Estin [52] has reported measurements on imprecise SMA connectors, but used a method which is applicable to any other connector type provided that all discontinuities within the pair are not displaced from each other along the transmission line by a significant phase shift, hence, applies to connector pairs that can be described as single two-ports. This approach does not require the assumption that all connectors of the type are identical, but measures a hypothetical composite pair that comprises the two connectors under test which are mounted at each end of the test line. These connectors must either be sexless, or of opposite sex. In this method effects of the system connectors are eliminated to first order. The imperfections of the artifact reference standards are also eliminated to first order, so it is not necessary that the short-circuit and matched-load standards be of standards laboratory quality or be calibrated.

Time-domain measurement is a potentially valuable tool for determining connector properties. Present techniques include both direct time-domain analyzers, which use generators and detectors having response times as low as a few picoseconds, and broadband frequency-domain analyzers with FFT software. Both approaches are well able to separate the physical effects of a connector pair from the adjacent circuitry, but the resolution of fine quantitative detail in the scattering parameters (in the frequency range above 10 GHz) is limited, as is the accurate determination of losses in the pair of connectors under test.

2.4 *New work: present and future*

Efforts to improve microwave power standards generally consist of microcalorimeter refinements that reduce the uncertainty and speed up the measurement,

or extend the measurement to higher frequencies in new types of transmission line configurations such as 3,5 mm and 2,4 mm coax.

The evaluation of a coaxial microcalorimeter for coaxial power standards has been difficult and limited because the center conductor is isolated from the thermopile. A new technique has improved the ability to correct the measurement for heat loss through the center conductor. Automation and other refinements have reduced the measurement time so that direct measurement of the effective efficiency of a customer's mount in the microcalorimeter is a practical possibility. This can let the customer have a transfer standard with an uncertainty as good as the internal working standard used by the standards laboratory itself.

Microwave systems that operate above 18 GHz using new smaller coaxial lines and connectors are in common use. Hence, the need for power standards with these connectors has arrived, but without the degradation in accuracy resulting from measuring through adaptors. Development on new dc-substitution detectors, mounts, and microcalorimeters in 3,5 mm and 2,4 mm coax that can meet that need is starting. New techniques for direct temperature measurement in microcalorimeters are under development. These techniques may eliminate the need for nanovolt dc measurements and their attendant sources of noise and instability.

3. Thermal Noise Measurement Technology (J. Wayde Allen)

3.1 Introduction

The development of new, very-low-noise amplifiers and the increasing complexity of today's microwave systems have increased demands on high-frequency engineering measurement capabilities. However, the thermal noise of the devices themselves remains a fundamental limitation to the performance of these new systems. Consequently, there is a growing need for accurate noise measurement methods, systems, and standards. The purpose of this section is to provide a brief overview of the current state of the art in thermal noise measurement technology as represented principally by that at the NIST.

3.2 Noise measurement systems

Thermal noise is the result of random fluctuations in the quantum energy of matter and is better known as black-body radiation. This means that all objects at temperatures above absolute zero radiate energy in the form of electromagnetic waves [53-56]. Many different tyes of radiometer systems have been built to detect this energy [57], although not all of these receivers lend themselves well to precise noise metrology. The basic requirement behind the design of a radiometer used to provide thermal noise calibration services is for a system that has three characteristics: (i) sufficient sensitivity to detect the noise power from the sources to be measured; (ii) adequate stability over the course of the measurement; and (iii) a means of comparing the noise output from some unknown source to that of at least one known source. Since the components making up the radiometer themselves generate noise, these requirements are not trivial.

Further, the impedance match between the radiometer and the noise source being measured affects the power transfer from the source to the radiometer. Thus the impedance mismatch between the unknown source and the radiometer and that between the calibration standard and the radiometer must be taken into account. At the NIST, three different techniques have been used to satisfy this impedance condition. The first of these is to tune the radiometer input in such a way that the noise power from the source is delivered to a reflectionless load. The second technique is to tune the impedance of the calibration standard to match the impedance of the unknown source [58]. This forces the impedance mismatches that the calibration standard and the unknown device present individually to the radiometer to be equal. Since the measurement depends on a comparison between these sources, the mismatch drops out. The third technique is to measure the impedance mismatch between the radiometer and each of the sources and to correct for it analytically.

In order to meet these radiometer requirements, the NIST currently employs two radiometer designs. The first of these is a modified Dicke (switching) radiometer system, which has served as the most commonly used radiometer since the 1960s. Basically the Dicke radiometer is a comparison radiometer whose input is switched at an audio frequency between two different noise sources. The output envelope from the radiometer power detector is consequently modulated at the switching speed and has a magnitude related to the difference between the powers of the two input noise signals.

In the NIST switching radiometer, an uncalibrated but stable power noise source is used as a comparison reference at port 1 of the switch. Port 2 is the actual measurement port to which both the standard noise source and the DUT are successively attached. Port 2 is manually tuned to act as a reflectionless load. The measurement is accomplished by first placing a standard noise source cascaded with a calibrated attenuator at port 2. The calibrated attenuator is adjusted until the averaged powers at the two ports are equal. Once this has been done, the unknown noise source may be attached in place of the standard noise source and the attenuator readjusted to again minimize the amplitude of the switching envelope.

The difference in the attenuator settings allows the noise power that the unknown device will deliver to a reflectionless load to be calculated with reference to the noise power of the known standard. The main disadvantages of this kind of radiometer are: (i) the switch must be repeatable to the desired measurement accuracy; (ii) the manually tuned input port restricts the system to measurements at only a single frequency at a time; and (iii) this system does not lend itself well to computerized data collection. For these reasons, current plans at the NIST call for the retirement of the Dicke radiometer systems within the next two years. For a more complete description of design and error analysis of the Dicke radiometer system, see the existing literature [59-62].

The second design is an automated total power radiometer. These new systems were specifically designed to automate the measurement by eliminating the need to manually tune the input impedance of the radiometer. This was accomplished by designing the system to include a six-port network analyzer [63] as an integral part of the radiometer's front end. This gives the system the capability of directly measuring the reflection coefficients of the noise sources being measured and hence permits analytic calculation and exact compensation of the resulting mismatch. Also, since the six-port can be calibrated at many frequencies, this correction makes it possible for the radiometer to measure the noise source over a broad frequency band. Automation of the power measurement was accomplished by eliminating null-type power detection and relying on a mathematical model of the electrical properties of the detector in order to relate the incident rf power to the dc voltage of the detector [64, 65]. Referring to the block diagram in Figure 9, the radiometer contains a front-end switch which allows the operator to select between an ambient (300 K) noise source, a cryogenic (78 K) noise source, and the source being measured. This switch is followed by a directional coupler which, when switch 1 is set to make six-port measurements, couples some of the rf power from the local oscillator (G) to the front of the radiometer. This makes it possible for the six-port to measure the reflection of the input ports of the radiometer and at the same time assures that the noise and reflected six-port probe powers are directed through the directional coupler and rf amplifier to switch 2. Setting switch 1 to supply the local oscillator power to the six-port and switch 2 to direct the reflected probing wave to the six-port junction makes the system function as a six-port network analyzer. On the other hand, if switches 1 and 2 are set to connect the local oscillator and rf paths to the mixer, the system is configured as a high gain superheterodyne radio receiver whose output power is a function of carefully stabilized system temperature and the noise power at the selected radiometer test port. This makes a comparison between the noise

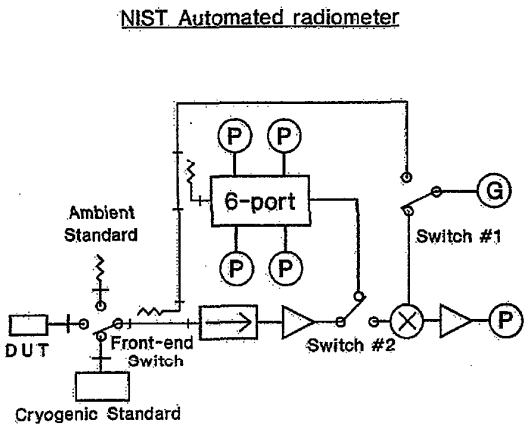

Figure 9. Block diagram of the NIST automated radiometer.

powers seen at the system's input test ports possible, but of course assumes that the insertion losses of the input paths are identical.

Making a measurement with this system involves three basic steps. The first is to calibrate the built-in six-port network analyzer at the input test ports. The second is to determine any differences in the rf path insertion loss between the input ports (asymmetry evaluation). The third step measures the output powers of the radiometer corresponding to inputs of the two known standards and the DUT.

The six-port calibration is the basic single six-port calibration that was developed by Engen [66] and uses a short circuit whose complex reflection coefficient is known, a sliding short circuit, and a sliding load. This calibration, which is outlined in Section 1 of this paper, is followed for all of the radiometer input ports except the ambient standard port at each of the frequencies needed. (No six-port measurements are needed for the ambient standard port as the radiometer is maintained at the same ambient temperature. An impedance mismatch has no effect in this special case because the power spectral density on both sides of the reference plane are the same. Thus, the ambient standard need never be disconnected from the radiometer system.)

The port asymmetry measurement is the next part of the system calibration. It is usually determined by connecting two different noise sources to the radiometer's input ports, measuring the resulting radiometer output power, interchanging the two sources, remeasuring the radiometer's output power, and comparing the results. This method [67] does not provide enough information to calculate the exact path efficiencies but it does allow us to calculate the path efficiency ratio η_s/η_x betwen the paths tested. The subscripts s and x refer to the cryogenic standard and

DUT input ports, respectively. It is sufficient to correct the measured radiometer powers for the insertion loss differences between the input ports.

After the first two steps have been completed, the radiometer system itself is calibrated, and comparison measurements between the three input noise sources may be made. The cryogenic standard and the DUT are then in turn connected to the remaining radiometer input ports, and the six-port is used to measure their complex reflection coefficients. These data are combined with the complex reflection coefficients obtained by the six-port calibration for the input ports of the radiometer to obtain values for the associated mismatches between the radiometer M_x and the noise sources M_s. (Again, the subscripts s and x refer to the cryogenic and DUT port mismatches, respectively.) At this point, all that remains is to measure the radiometer's output powers P_a, P_s and P_x associated with the ambient standard temperature (T_a), the cryogenic standard temperature (T_s), and the unknown standard temperature (T_x), respectively. These powers are then used to form the Y-factors $Y_x = P_x/P_a$ and $Y_s = P_s/P_a$ from which the unknown temperature T_x is calculated using [67],

$$T_x = T_a + \left(\frac{M_s \eta_s}{M_x \eta_x}\right)\left(\frac{Y_x - 1}{Y_s - 1}\right)(T_s - T_a). \qquad (8)$$

For a measurement of a different device at the same frequencies, it is necessary only to connect it to the DUT port and repeat the last six-port and power measurement sequence in order to obtain a value for T_x.

3.3 *Noise standards*

All of the noise measurement systems discussed would be essentially useless without some noise source whose temperature is accurately known. Possibilities for such sources include black-body radiators, gas discharge tubes and avalanche noise diodes. However, the noise output from sources such as gas discharge tubes and diodes cannot generally be computed to a high accuracy and is best determined experimentally. Since this means that their noise outputs must be compared against some other known noise source, such devices do not make good primary standards [59, 60]. They are, however, robust noise sources with high output of good stability. Moreover, they are physically small and easily maintained. Although the noise output powers are somewhat sensitive to ambient temperature, they are extensively used in the field as transfer standards. The main usefulness for a noise calibration capability in a primary standards laboratory is the calibration of the noise output from such devices.

The black-body radiator lends itself well as a primary standard since the calculation of its radiated power spectral density is by the well-known Planck radiation law [54, 55, 56]. An effective microwave black-body radiator can be constructed of a variety of stable materials in different configurations. Its "blackness" can be evaluated with a network analyzer by using the equivalence of emissivity and absorptivity as stated in Kirchhoff's law. The major difficulty with such a standard lies in its temperature control. The most common methods either use a resistive heating element and a temperature sensor connected through a feedback control network, or rely on some physical phase transition such as the melting point of water or the boiling point of nitrogen to maintain the black body at a well-known temperature [58]. The attainable accuracy of any one of these temperature control schemes is, however, heavily dependent on the physical design and construction of the standard. Both the mounting structure for the load and the transmission line used to connect the standard to the radiometer have finite thermal conductivities which must be understood if the true temperature of the standard is to be known, and any inhomogeneities in the load configuration may preclude the establishment of a uniform temperature profile. The materials making up the standard must also be stable at the temperatures used. This is an especially significant problem for the high-temperature loads where the solid solubility of the dissimilar materials comprising the standard may become important. The diffusion of one material into another can significantly alter the overall electromagnetic properties of the device.

The NIST currently uses a liquid-nitrogen-cooled cryogenic load which is designed in such a way as to be a self-regulating system [68, 69]. Figure 10 is a schematic drawing of this kind of waveguide standard [69]. A series of silicon carbide wedges forms the black-body source at the bottom of a cavity designed to shield the standard from external sources of radiated noise power. A waveguide horn antenna is mounted at the top of this cavity and is used to couple the radiated power from the silicon carbide load into the waveguide output from the standard. Temperature regulation of this standard is achieved through the natural heat pipe action of the liquid nitrogen in concert with the porous silicon carbide ceramic. This occurs when the Dewar in which the standard black-body cavity is located is filled with liquid nitrogen so that only the bottom part of the silicon carbide load is immersed. The silicon carbide then acts like a sponge, with the liquid nitrogen being wicked up onto the surface of the vanes where it boils off. This continuous wicking action maintains the surface temperature of the load material at the boiling point of liquid nitrogen. Determination of the working temperature of the standard is then achieved by measuring the barometric pressure, calculating the boiling point of liquid nitrogen from the vapor pressure equation and correcting this temperature for the noise contribution of the shielding cavity and

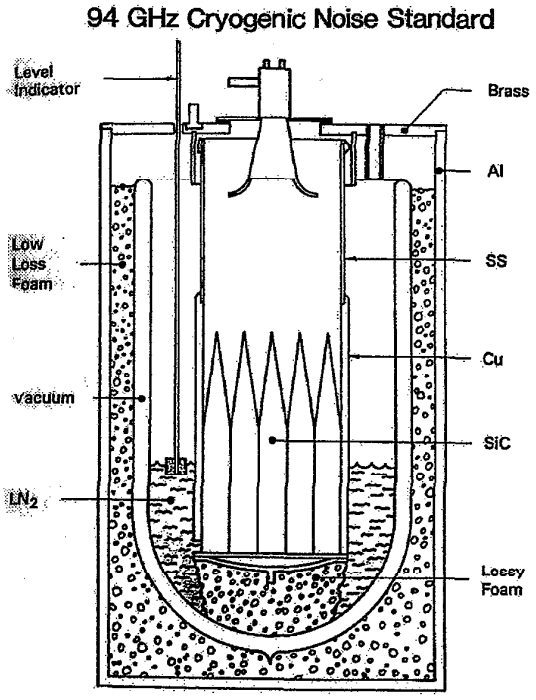

Figure 10. The NIST WR-10 noise standard.

waveguide horn [67, 68]. Not only has this proved to be a highly effective approach to the design of a stable cryogenic black-body standard, but it has also eliminated the errors as well as the added complexity and maintenance problems associated with the feedback and control circuitry inherent in many of the other black-body standard designs.

3.4 The future of noise measurements

The development of the NIST's new automated radiometer system and the self-contained cryogenic standard has brought new flexibility to noise measurements. For example, the means are available to make measurements of a noise source at several frequencies simultaneously. We anticipate that this automated capability will make noise calibration services more economical and faster in the near future. This capability combined with plans to offer noise calibration services spanning a frequency range from 10 MHz to 110 GHz in the next five years is expected to make true broadband noise standard calibrations possible.

The drive towards broadband frequency coverage has also meant that the measurement systems must be compatible with a greater number of connector types. This has led to the development and application of techniques allowing for the precise measurement of noise sources through various types of adaptors [70, 71]. Basically, the problem with making a comparison between noise sources having different connector types has to do with the ability to characterize the adaptor connecting the device to the system. Since the NIST's new radiometer is built with multiple input ports it is not a problem to connect the primary standard in the usual fashion and to attach the DUT through an adaptor. Hence, if the necessary standards are available to calibrate the six-port on the DUT side of the adaptor, it is still possible to determine the reflection coefficient between the DUT and the adapted radiometer input port. However, the problem lies in determining the difference between the insertion loss of the path connecting the primary standard to the system and the signal path through the DUT input port. As stated above, the most common method of determining this path asymmetry is to connect two sources to the two different input ports and measure the associated powers, then to reverse the devices relative to the ports and measure the powers again. This procedure gives a ratio of path efficiencies, which is enough information to correct for the fractional power difference between the two paths. Since the connector type is different on the two ports, such methods can no longer be used for the through-adaptor case. However, a separate six-port calibration is performed on each of the input ports. If the two paths are identical the calibration constants obtained for each of the six-port calibrations should in fact be equal. If, however, the paths are different, then the six-port calibration constants for each of the input ports will reflect this difference. Consequently, calibrating the six-port at each of the input ports provides the information needed and makes the characterization of the adaptor used for the measurement essentially transparent to the operator. This is a powerful technique in that it makes it possible to compare any noise source, regardless of its connector type, directly to primary noise standards.

Amplifiers with extremely low values of noise figure have approached the limits of the existing measurement techniques, and have prompted the NIST to begin work towards developing new noise figure calibration services [72]. This work, along with an effort to lower the uncertainty of the existing calibration services, should make it possible to determine the noise figure of these low-noise amplifiers with even greater accuracy.

References

1. Adam S. F., *Microwave Theory and Applications*, Englewood Cliffs, NJ, Prentice Hall, Inc., 1969.
2. Hoer C. A., A network analyzer incorporating two six-port reflectometers, *IEEE Trans. MTT*, 1977, **MTT-25**, 1070-1074.

3. Engen G. F., An improved circuit for implementing the six-port technique of microwave measurements, *IEEE Trans. MTT*, 1977, **MTT-25**, 1080-1083.
4. Cronson H. M., Susman L., A six-port automatic network analyzer, *IEEE MTT-S International Microwave Symposium Digest*, 1977, 50-52.
5. Speciale R., Analysis of six-port measurement systems, *IEEE MTT-S International Microwave Symposium Digest*, 1979, 63-68.
6. Somlo P. I., Hunter J. D., A six-port reflectometer and its complete characterization by convenient calibration procedures, *IEEE Trans. MTT*, 1982, **MTT-30**, 186-192.
7. Hoer C. A., Using six-port and eight-port junctions to measure active and passive circuit parameters, *Nat. Bur. Stand. (US) Tech. Note 673*, 1975, 22 p.
8. Juroshek J. R., Hoer C. A., A dual six-port network analyzer using diode detectors, *IEEE Trans. MTT*, 1984, **MTT-32**, 78-82.
9. Colef G., Ettenberg M., Karmel P. R., Performance of an integrated six-port reflectometer operated with pulsed signals, *IEEE Trans. I & M*, 1990, **IM-39**, 195-200.
10. Demers Y., Bosisio R. G., Gannouchi F. M., Repetitive and single shot pulse microwave six-port reflectometer, *IEEE Trans. I & M*, 1990, **IM-39**, 195-200.
11. Colef G., Karmel P. R., Ettenberg M., New in-situ calibration of diode detectors used in six-port network analyzers, *IEEE Trans. I & M*, 1990, **IM-39**, 201-204.
12. Hoer C. A., Roe K. C., Allred C. M., Measuring and minimizing diode detector nonlinearity, *IEEE Trans. I & M*, 1976, **IM-39**, 324-328.
13. Chen Zhaowu, Binchun Xu, Linearization of diode detector characteristic, *IEEE MTT-S Symposium Digest*, 1987, **1**, 265-267.
14. Rytting D. K., Advances in microwave error correction techniques, *Hewlett-Packard RF and Microwave Symposium*, 1987.
15. Engen G. F., Hoer C. A., Thru-reflect-line: an improved technique for calibrating the dual six-port automatic network analyzer, *IEEE Trans. MTT*, 1979, **MTT-27**, 983-987.
16. Renmark S., On the calibration process of automatic network analyzer systems, *IEEE Trans. MTT*, 1974, **MTT-22**, 457-458.
17. Franzen N. R., Speciale R. A., A new procedure for system calibration and error removal in automated S-parameter measurements, *Proc. 5th European Microwave Conf.*, 1975, 69-73.
18. Beatty R. W., Calculated and measured S_{11}, S_{21}, and group delay for simple types of coaxial and rectangular waveguide 2-port standards, *Nat. Bur. Stand. (US) Tech. Note 657*, 1974, 2 p.
19. Hoer C. A., On-line accuracy assessment for the dual six-port ANA: treatment of systematic errors, *IEEE Trans. I & M*, 1987, **IM-36**, 514-519.
20. Marks R. B., A multiline method of network analyzer calibration, *IEEE Trans. MTT*, 1991, **MTT-39**, 1205-1215.
21. Marks R. B., Williams D. F., Characteristic impedance determination using propagation constant measurement, *IEEE Microwave and Guided Wave Letters*, 1991, **1**, 141-143.
22. Heinrich W., Full-wave analysis of conductor losses on MMIC transmission lines, *IEEE Trans. MTT*, 1990, **38**, 1468-1472.
23. Williams D. F., Marks R. B., Transmission line capacitance measurement, *IEEE Microwave and Guided Wave Letters*, 1991, **1**, 243-245.
24. Fantom A., Power and energy: national standards, *Proc. IEEE*, 1986, **74**, 94-101.
25. Fantom A., *Radio Frequency and Microwave Power Measurement*, London, Peter Peregrinus Ltd., 1990, 115 p.
26. Clague F. R., The NIST automated coaxial microwave power standard, *Proc. Measurement Science Conf.*, 1989.
27. Larsen N. T., A new self-balancing dc-substitution rf power meter, *IEEE Trans. I & M*, 1976, **IM-25**, 1-12.
28. See Fantom A., *Radio Frequency and Microwave Power Measurement*, London, Peter Peregrinus Ltd., 1990, Ch. 10, for specific references.
29. McPherson A. C., Kerns D. M., A microwave calorimeter, *Rev. Sci. Instrum.*, 1955, **26**, 27-33.
30. Clark R. F., The microcalorimeter as a national standard, *Proc. IEEE*, 1986, **74**, 102-104.
31. Fantom A., *Radio Frequency and Microwave Power Measurement*, London, Peter Peregrinus Ltd., 1990, 20.
32. Fantom A., *Radio Frequency and Microwave Power Measurement*, London, Peter Peregrinus Ltd., 1990, 28.
33. Clark R. F., Jurkus A., Ten watt coaxial calorimeter for rf power measurement, *Rev. Sci. Instrum.*, 1968, **39**, 660-665.
34. Yokoshima I., Development and design of calorimeter type microwave power meter for the frequency range 60-90 GHz, *NPL Report DES 22*, 1973.
35. Vowinkel B., Broad band calorimeter for precision measurement of millimeter and submillimeter wave power, *IEEE Trans. I & M*, 1980, **IM-29**, 183-189.
36. Keen N. J., Milliwatt calorimeter for the 90-140 GHz waveguide band, *Electron. Lett.*, 1984, **10**, 384-385.
37. Aoki T., Ohi K., Ueki K., Some studies in behaviour of microwave dry calorimeter, *Hitachi Rev.*, 1969, **18**, 235-240.
38. Fantom A., *Radio Frequency and Microwave Power Measurement*, London, Peter Peregrinus Ltd., 1990, 47.
39. Skilton P. J., Developments in United Kingdom waveguide power standards, *RSRE Report 80006*, 1980.
40. Clague F. R., The NIST automated coaxial microwave power standard, *Proc. Measurement Science Conf.*, 1989.
41. Beatty R. W., McPherson A. C., Mismatch errors in microwave power measurements, *Proc. IRE*, 1953, **41**, 1112-1119.
42. Engen G. F., Beatty R. W., Microwave reflectometer techniques, *IRE Trans. MTT*, 1959, **MTT-7**, 351-355.
43. Engen G. F., A transfer instrument for the intercomparison of microwave power meters, *IRE Trans. I & M*, 1960, **I-9**, 202-208.
44. Harris I. A., An accurate method for the comparison of two RF power meters which have similar or differing power ranges, *Progress in Radio Science* 1966-69 (Edited by J. A. Lane, J. W. Findlay and C. E. White), Brussels, URSI, **2**, 249-254.
45. Oldfield L. C., Ide J. P., Measurement of complex reflection coefficients in W-band using a 4-port reflectometer and precision waveguide spacers, *IEE Colloquium*

on Advances in S-Parameter Measurement at Millimetre Wavelengths, London, 1983, 8/1-8/6.
46. Adam S. F., Automatic microwave network measurements, *Proc. IEEE*, 1978, **66**, 384-391.
47. Engen G. F., Hoer C. A., Application of an arbitrary 6-port junction to power measurement problems, *IEEE Trans. I & M*, 1972, **IM-21**, 470-474.
48. IEEE G-IM Subcommittee on Precision Coaxial Connectors, Precision coaxial connector coupling mechanisms, contact designs, and higher mode resonances, *IEEE Trans. I & M*, 1968, **IM-17**, 219-222.
49. IEEE Standard for precision coaxial connectors, *IEEE Trans. I & M*, 1968, **IM-17**, 206-218.
50. Beatty R. W., Engen G. F., Anson W. J., Measurement of reflections and losses of waveguide joints and connectors using microwave reflectometer techniques, *IRE Trans. Instrum.*, 1960, **I-9**, 219-226.
51. Harris I. A., Mode of use and assessment of precision coaxial connectors, *Proc. IEE*, 1965, **112**, 2025.
52. Estin A. J., Scattering parameters of SMA connector pairs, *IEEE Trans. I & M*, 1976, **IM-25**, 329-334.
53. Bell D. A., *Electrical Noise Fundamentals and Physical Mechanism*, London, D. Van Nostrand Company Ltd., 1960, 37-87.
54. Kraus J., *Radio Astronomy*, 2nd ed., Powell, Ohio, Cygnus-Quasar Books, 1986, 3-19 to 3-43.
55. Kittel C., Kroemer H., *Thermal Physics*, 2nd ed., San Francisco, W. H. Freeman & Co., 1980, 89-102.
56. Gasiorowicz S., *Quantum Physics*, New York, John Wiley & Sons, 1974, 1-7.
57. Kraus J., *Radio Astronomy*, 2nd ed., Powell, Ohio, Cygnus-Quasar Books, 1986, 7-0 to 7-72.
58. Wait D., Nemoto T., Measurement of the noise temperature of a mismatched noise source, *IEEE Trans. MTT*, 1968, **MTT-16**, 670-675.
59. Estin A. J., Trembath C. L., Wells J. S., Miller C. K. S., Absolute measurement of microwave noise sources, *IEEE Trans. Instrum.*, 1960, **I-9**, 211-213.
60. Miller C. K. S., Daywitt W. C., Arthur M. G., Noise standards, measurements, and receiver noise definitions, *Proc. IEEE*, 1967, **55**, 865-877.
61. Wells J. S., Daywitt W. C., Miller C. K. S., Measurement of effective temperatures of microwave noise sources, *IEEE Trans. I & M*, 1964, **IM-13**, 17-28.
62. Wait D. F., Sensitivity of the Dicke radiometer, *J. Res. Nat. Bur. Stand. (US)*, 1967, **71C**, 127-152.
63. Engen G. F., The six-port reflectometer: an alternative network analyzer, *IEEE Trans. MTT*, 1977, **MTT-25**, 1075-1079.
64. Montgomery C. G., *Technique of Microwave Measurements*, MIT Radiation Laboratory Series, New York, McGraw-Hill Book Company, Inc., 1947, 79-218.
65. Larsen N., NBS Type IV rf power meter operation and maintenance, *Nat. Bur. Stand. (US) NBSIR*, 1977, 77-86.
66. Engen G. F., Calibrating the six-port reflectometer by means of sliding terminations, *IEEE Trans. MTT*, 1978, **MTT-26**, 951.
67. Daywitt W., Radiometer equation and analysis of systematic errors for the NIST automated radiometers, *Nat. Inst. Stand. Technol. Tech. Note 1327*, 1989.
68. Daywitt W., Design and error analysis for the WR10 thermal noise standard, *Nat. Bur. Stand. (US) Tech. Note 1071*, 1983.
69. Daywitt W., A coaxial noise standard for the 1 GHz to 12.4 GHz frequency range, *Nat. Bur. Stand. (US) Tech. Note 1074*, 1984.
70. Engen G. F., A method of calibrating coaxial noise sources in terms of a waveguide standard, *IEEE Trans. MTT*, 1969, **MTT-16**, 636-639.
71. Daywitt W., Billinger R., A simple method for measuring adapter efficiency, *Microwave Journal*, to be published.
72. Wait D. F., Engen G. F., Application of radiometry to the accurate measurement of amplifier noise, *IEEE Trans. I & M*, 1991, **IM-40**, 433-437.